**Supporting Information**

**Experimental Details:**

## 1. Synthesis of Silver Nanoparticles

Silver nitrate (>99%) and trisodium citrate dihydrate (99.0%) were purchased from Aldrich. All descriptions of water below refer to Nanopure deionized water (electrical resistance >18.4 MΩ-cm), produced from a Barnstead Nanopure® water system. Silver nanoparticles were prepared by citrate reduction of silver nitrate. $AgNO_3$ (17.0 mg) was dissolved in 100 mL water in a 250 mL tri-neck flask. The solution was heated to boiling with a hemisphere heating mantle under vigorous magnetic stirring. After boiling for 2 minutes, an aqueous solution of sodium citrate (35 mM, 10 mL) was rapidly added to the flask. The solution gradually turned yellow within a few minutes, indicating the formation of Ag nanoparticles. The solution was kept boiling for an additional 6 minutes. After that, the heating mantle was removed, and the solution was allowed to cool.

TEM imaging of the nanoparticles was carried out with a Tecnai F30 STEM/TEM microscope, which is equipped with a thermal Schottky field emission gun and operates at 300 kV. Images are acquired with a 4096x4096 pixel CCD (Gatan; pixel resolution for images in Figure 1 (zoom-in images) and Figure 3 is 0.5 nm). The as-prepared Ag colloids typically consist of a majority (~90%) of nearly spherical nanoparticles with an average diameter ~50 nm (standard deviation ~ 20%) and a fraction (5~10%) of nanorods with various aspect ratios.

## 2. SH Measurements and Data Processing

A specially designed $Si_3N_4$ window TEM grid (3 mm diameter Si substrate with a 0.2 m x 0.2 mm central square window) was used in our work. The position markers on the window were fabricated by standard electron-beam lithography. The $Si_3N_4$ substrate was first coated with a thin layer (8 nm) of silicon monoxide via thermal evaporation in order to change the hydrophobic nature of the $Si_3N_4$ surface to hydrophilic. The substrates were then spin-coated with electron resist (a double layer of MMA-MAA copolymer and PMMA-950 polymer), followed by electron-beam writing. The patterned substrate was further deposited with a thin layer (20 nm) of chromium to act as the marker material, followed by liftoff in acetone.

The $Si_3N_4$ window on the Si substrate with Cr bar-markers (1 μm x 9 μm) were immersed in an aqueous solution of a positively charged PDDA polymer (polydimethyldidodecylammonia chloride, low Mw, Aldrich) for ~10 hours, resulting in the deposition of a layer of PDDA polymer onto the window surface. The substrate was rinsed with water and dried. A 5 μL aliquot of Ag colloidal solution (diluted 1:4 with water) was pipetted onto the window and allowed to stand for approx. 5-10 minutes for particle deposition via electrostatic interaction (note that Ag nanoparticles are negatively charged), then rinsed with water and dried. The $Si_3N_4$ substrate bearing Ag nanoparticles was taped onto a glass coverslip (180-190 μm in thickness) that was positioned above the objective lens.

SH activity maps were generated by raster scan over the sample with a tightly focused (diffraction limited) beam with a home-built nonlinear imaging microscopy system based on an

inverted optical microscope (Nikon TE 2000) and a Titanium:Sapphire femtosecond pulsed laser system (Spectra Physics Mai-Tai Broadband). After spatially filtering, tunable 100fs duration pulses (80 MHz) from the source were dispersion precompensated with a BK7 Brewster-cut prism pair (R. Matthews). To minimize beam walk (unavoidable when changing wavelengths), two closed-loop voice-coil beam stabilizer mirrors (Optics In Motion) were used to remove pointing jitter and precisely lock the alignment. Two beam samplers and position sensitive photodiodes completed the feedback loop. A galvanometer (Cambridge Technology 6650), imaged at the back focal plane of a 60x 1.4 NA oil-immersion objective (Nikon) by a scan lens and tube lens that also served to expand the beam to overfill the objective back aperture, raster scanned the beam over the sample. A closed-loop xyz piezo scan stage (PI-561) provided fine sample translation and focusing. A dichroic shortpass mirror (Chroma 675DCSPXR4), bandpass filter (Chroma HQ450/100m), and two-photon blocking filter (Chroma E700-sp2) separated the epi-scattered SH signal that was projected onto a 1000x1000 pixel electron-multiplying cooled CCD (Andor DV-885) with a 1.5x slider for a total magnification of 90x and an effective image size per pixel of 88.9nm. Images were acquired with an integration time of 2.5 seconds and averaged over 40 frames.

Prior to the SH activity measurements, a bright field image of the marked area of the sample was first acquired with white light (i.e. halogen) condenser illumination. After that, the sample position was fixed and the femtosecond NIR laser pulses were introduced and careful adjustment of the focus was conducted to ensure maximum SH signal from Ag nanoparticles. For each sample, SH measurements were conducted for various excitation wavelengths, laser power and polarizations. The SH emission spectrum was acquired with a Triax 320 spectrometer and an Andor DU 420-OE CCD. TEM imaging was done both prior to and after SH measurements.

SH image data processing was done with *ImageJ* software (version 1.33, downloaded from National Institute of Health USA website, http://rsb.info.nih.gov/ij/). A specific area of interest (typically 5-10 um in size) in the SH activity map was cropped out and matched with the corresponding TEM image of the same area. Individual Ag nanoparticles were then identified in both images allowing direct particle-specific correlation.

## 3. Supporting Schemes

**Scheme S1.** (A) The two-photon nonlinear optical microscopy system used in this work. (B) depicts the epi-illumination/detection geometry.

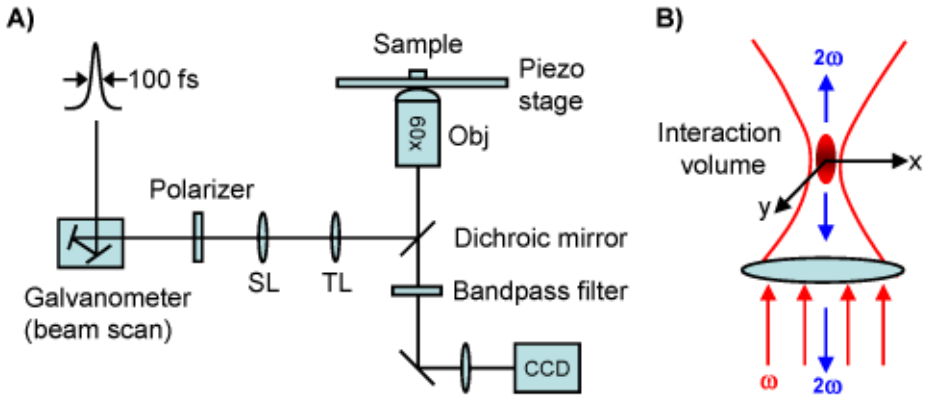

**Scheme S2.** (A) Conventional SHG mechanism versus (B) the proposed mechanism for SH from one-photon driven plasmon polarization response. The excitation spectral, power and emission dependence and the correlation with specific structures of the single nanoparticles (or dimers, trimers, etc.) all point to a one-photon resonant mechanism. The large local-field from the resonance (and high laser peak power density) strongly suggest that the highly driven plasmon leads to significant nonlinearity in the material polarization. This results in considerable SH activity - 100 fold more than from single spherical particles.